Vibration-Based Fault Detection of Accelerometers in Helicopters

Victor Girondin, Mehena Loudahi, Komi Midzodzi Pekpe, Jean Philippe Cassar

Vibration-based fault detection of accelerometers in helicopters

Victor Girondin [*,**] **Mehena Loudahi** [**] **Herve Morel** [*]
Komi Midzodzi Pekpe [**] **Jean-Philippe Cassar** [**]

[*] *EUROCOPTER F-13725 Marignane Cedex, France*
[**] *LAGIS - UMR CNRS 8219 Université Lille 1 Boulevard Langevin 59655 Villeneuve d'Ascq*

Abstract: Vibration-based monitoring is an approach for health analysis of helicopters. However, accelerometers and other sub-elements that convert and transmit vibrations to the recording system must not corrupt the signal. These elements are prone to defects because of external injuries during flights or maintenance. This paper will deal with a method to tackle problems of loosening and mechanical shocks. The objective is to perform a passive detection of accelerometer failures from the vibrations without knowledge of previous recordings. Experiments of mechanical failures have been carried out on a shaker to reproduce in flight vibrations, and it appears that the loosening and mechanical shocks introduce asymmetry and random peaks in the temporal vibrations. Loosening was successfully detected but mechanical shocks were much harder to detect as a result of strong dependences in the vibratory environment. Loosening data sets from flights confirm experimental observations and the proposed detection method allows for the detection of the fault with better performance than standard indicators.

Keywords: accelerometers; vibration; helicopter; monitoring; skewness; HUMS

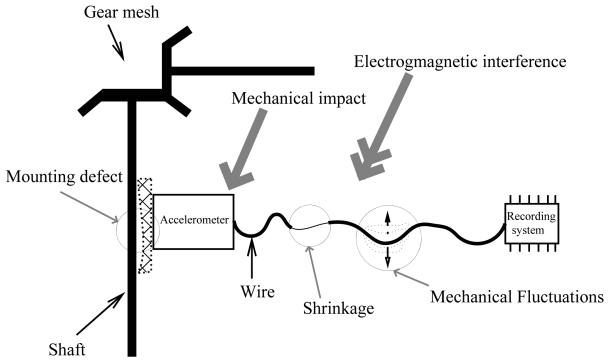

Fig. 1. Example of components and failures of an information chain.

1. INTRODUCTION

According to Eurocopter HUMS [1] Support, more than 50% of false alarms are due to failures in the information chain of helicopters between the mechanical system and the recording system. This part is prone to different kinds of failures, resulting in various impacts on the signal: additive, multiplicative or convolutive interferences. Figure 1 presents different faults that can act on the path of generation and transmission of accelerometer information. Indeed, an accelerometer is failing when one component in its path is failing.

Some defects different in nature are presented on figure 1.

The impact of defects can be more noticeable in:

- *time domain*: aberrant values, unstationnary fluctuations, flat or nearly zero outputs. Possible origins are overheating, mechanical impact...
- *frequential domain*: loss or gain of energy in a large band and parasitical poles or sources. Possible roots are mechanical impacts, wire fluctuations, changes in the mechanical impedance of the mounting...

Since, most of the encountered and identified causes of defects are loosening and mechanical shocks, this paper will focus on an algorithm to detect these two failures. These failures occur most of the time because of wrong gauging or hard flight vibratory context. Statistical indicators have been widely used among the HUMS community to monitor deviation from a normal state (Stewart [1977]).

However, some of these indicators (RMS, peak-to-peak ratio...) are not reliable, producing many false alarms and useless maintenance actions. Indeed, these indicators do not take into account the asymmetry induced by the faults in the statistics of the signal. On the contrary, this paper will exploit the property to design a new indicator.

First, the experimental setting will be presented as well as the two faults that are investigated. Then the proposed indicator will be described. The next section discusses the results on the shaker and on flight.

2. EXPERIMENTAL SETTINGS

2.1 Simulation of flight data

Several experiments have been carried out in the LAGIS laboratory to investigate consequences of accelerometers

[1] Health Usage and Monitoring Systems

Fig. 2. Picture of the shaker and of the recording system. 1: Computer, 2: dSPACE, 3: conditioner, 4: accelerometer, 5: preamplifier, 6: shaker.

defects: loosening, fall, overheating, wire squashing, over-tightening. The data used for the experiments have been selected from different flights of a helicopter and correspond to 3 sensor samplings at 48kHz, located at the epicyclic gearing (EPI), the main gearbox (MGB) and the tail drive shaft (TDS). These vibrations were reproduced at 48kHz via a computer-controlled shaker. The control system is made of one computer and one dSPACE controller board (DS1103 PPC Controller Board). A picture of the bench is presented in figure 2. Then the data was measured at 48kHz by an accelerometer mounted on the shaker. Synthetic data does not entirely match with the original data but the reproducibility is good enough in the [0;7000] Hz range.

Only the first two experiments (loosening and fall) produced exploitable results, since results from other experiments were either "on-off" or did not permit the observation of any changes (like over-tightening).

2.2 Loosenning

During this experiment, one accelerometer has been loosened gradually from it's mounting (starting at 2 Nm of nominal torque). The accelerometer has been unscrewed with two ranges of steps according to the loosening size: ~ 0.04 mm step before reaching 0.2 mm and then 0.1 mm step.

2.3 Falling

During this experiment, accelerometers have been released at increasing heights: from 50 cm to 230 cm with 20 cm step. The accelerometer has been replaced at 170 cm by a new accelerometer (checked during preliminary tests). Accelerometers have been released (free fall) on bitumen and visual inspections ensured that the accelerometer's pin was not affected.

3. PROPOSED INDICATOR

The figure 3 shows several examples of vibrations related to in-flight defects (loosening), the raw signals (a, c or e) are asymmetric with unidirectional pulses and the associated histograms remain nearly gaussian having a heavier side. Moreover, it is visible that the faulty vibrations

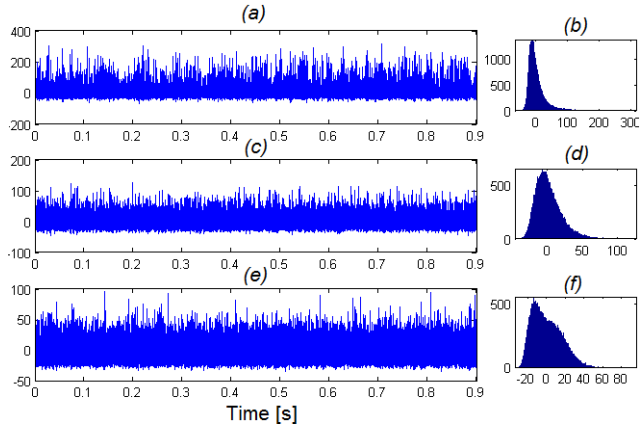

Fig. 3. The first column contain three raw signals from in-flight recordings. Only the first line corresponds to fault-free vibrations. The second column shows to the corresponding histograms.

are amplified for the positive values. To deal with such asymmetric signals, the third order normalized cumulant κ_3 is proposed as an indicator to detect the two faults:

$$\kappa_3 = E\left[\left(\frac{X}{\sigma}\right)^3\right] \tag{1}$$

Where X is a centered random variable with a density function p with standard deviation σ. In the second part of the paper, κ_3 is called the skewness. Skewness is legitimated for distributions that are nearly gaussians. According to Blinnikov and Moessner [1998] any probability density function can be decomposed using the Edgeworth asymptotic expansion with gaussian kernel. The first order expansion reveals the key roles played by κ_3 in the decomposition of p:

$$\begin{aligned} p(x) = & \frac{e^{-\frac{x^2}{2\sigma^2}}}{\sqrt{2\pi\sigma^2}} \\ & + \kappa_3^3 \times \frac{e^{-\frac{x^2}{(2\sigma^2)}}}{6\sqrt{2\pi\sigma^2}} \left(\left[\frac{x}{\sigma}\right]^3 - 3\left[\frac{x}{\sigma}\right]\right) \\ & + O(\sigma^2) \end{aligned} \tag{2}$$

As

$$\frac{e^{-x^2/(2\sigma^2)}}{6\sqrt{2\pi\sigma^2}} \left(\left[\frac{x}{\sigma}\right]^3 - 3\left[\frac{x}{\sigma}\right]\right) \tag{3}$$

is antisymmetric, the skewness expresses the influence of the anti-symmetric part of the signal. That decomposition is actually valid when p is a sum of random variables producing nearly-gaussian distributions. That hypothesis is verified, since histograms in figure 3 show that the vibrations can be seen as a sum of random variables producing a nearly gaussian distribution.

We propose to apply an optimized filter the vibrations to enhance skewness. This approach is an adaptation of the objective function method described by Lee and Nandi [2000] for blind deconvolution and applied by Endo and Randall [2007] for gear tooth fault detection. This solution has been selected considering its' stability and ease to be implemented.

3.1 Linear optimization of skewness

The best linear filter $b_1, b_2, ..., b_M$ to optimize the skewness of the filtered signal y_n from the raw data vib_n is the solution of the following optimization problem:

Model $y_n = b_1 \cdot vib_{n-1} + b_2 \cdot vib_{n-2} + \ldots + b_M \cdot vib_{n-M}$
Criterion find $[b_1, b_2, \ldots, b_M]$ so that the skewness of y_n is extremum

The iterative procedure to solve this optimization problem is described in Lee and Nandi [2000]. The output with optimized skewness is then the filtered signal y_n and the associated optimized skewness. A linear filter has been preferred rather than a non-linear filter because of its known-performance and stability. Moreover, it corresponds to an adaptive filtering of the frequencial bands where the skewness is stronger.

3.2 Algorithm and remarks

It appears that the mechanical defects of the accelerometer often create strong and directional pulses, which produce an exponential decrease in modulating the other vibrations, Serridge and Torben [1988] section 2.8. The characteristic time τ of the exponential decrease is associated with the low frequency limit of the accelerometer and is about 0.1 second.
Since, declines of peaks do not last longer than τ and occur randomly, the recording is split into τ-long segments to preserve local high values of skewness. An alarm is triggered when the maximum skewness over the segments exceeds a given threshold. The false alarm rate can be decreased by increasing the minimum number of different segments required to trigger an alarm. At last the algorithm is made of three steps:

(1) Filter the vibrations that optimize the skewness.
(2) Split the filtered signal into τ-long segments.
(3) Compute the skewnesses on the sub-segments.
(4) Raise an alarm if at least one segment exceeds a given threshold.

4. RESULTS

4.1 Experiments with shaker

For each experiment, optimized skewness is compared with standard skewness and the Spectral Kurtosis (Antoni [2007]) as it is a powerful tool for transient detection. Thresholds for spectral kurtosis, skewness and optimized skewness are set at 4, 0.2 and 0.5. These thresholds have been chosen to avoid false-detections while minimizing non-detection on the data sets of the experiments with shaker. In the following, optimized and standard skewnesses are expressed in terms of absolute value.

Loosenning Results are plotted in log-scale for readability purpose in figure 4. The three indicators have global similar shapes, which are "step-like fluctuations". It means that there is a loosening level to reach before the fault is observable: at 0.18 mm spacing, skewings and transients appear in the signal on figure 6. That highlights the non-linearity of mechanical system's behaviour. Spectral kurtosis allows detecting TDS and EPI after 0.18 mm, however

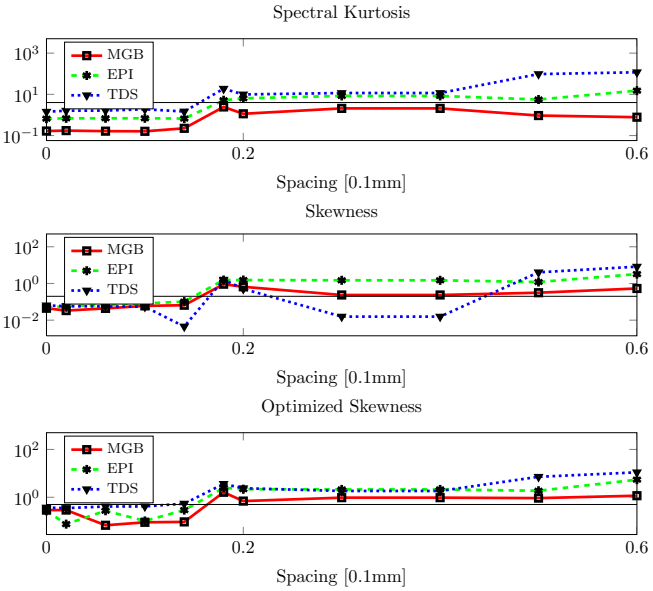

Fig. 4. Spectral Kurtosis, Skewness and Optimized Skewness in log-scale for loosening experiment. The spacing is in millimetres from the nominal position. Thresholds are plotted in solid line.

the MGB level after the failure is about TDS level before the overloosening limit (about 0.18 mm). Consequently MGB is not fully detected by the Spectral Kurtosis. (Standard) skewness detects EPI and MGB failures but not TDS for 0.3 and 0.4 mm. On the contrary, the optimized skewness detects TDS for these two values. TDS has been displayed at 0 mm and 0.3 mm in the figure 5. Actually the overall vibrations are slightly asymmetrical and for that reason skewness is not sufficient to reveal the faults. In figure, 6, the transients and the skewness are visually obvious for the 3 signals. The patterns look more like envelope modulations (multiplicative) for "EPI" whereas, they are impulsive for "MGB" and "TDS". Recordings from "EPI" reveal a directional force which depends on shaft rotation.

Falling Figure 7 shows the evolutions of the indicators according to the height of the falling. From figure 7, only TDS is prone to transients starting at 90 cm, probably because of high amplitude content at low frequencies (figure 8) that matches the characteristic time of decline associated with vibratory peaks ($1/\tau \sim 10$ Hz). Results tend to prove that for the main gearbox (MGB) and the epicyclic gearing (EPI), falling is much harder to detect because it is not excited by vibratory environment. As stated in the introduction, the fault may not be revealed depending on what kind of vibrations the accelerometers are subject to. For this reason, detectability differs from one vibratory environment to another. The power spectral density of the three recordings for normal states are displayed in figure 8, the fact that MGB and EPI do not have much spectral content in the low frequencies can explain poor reactions to the defect. There is an increase of 150 cm in figure 7, but the two indicators are then unsteady for TDS. The performances of the three indicators are poor because their values are significantly different from 0 only for 230 cm.

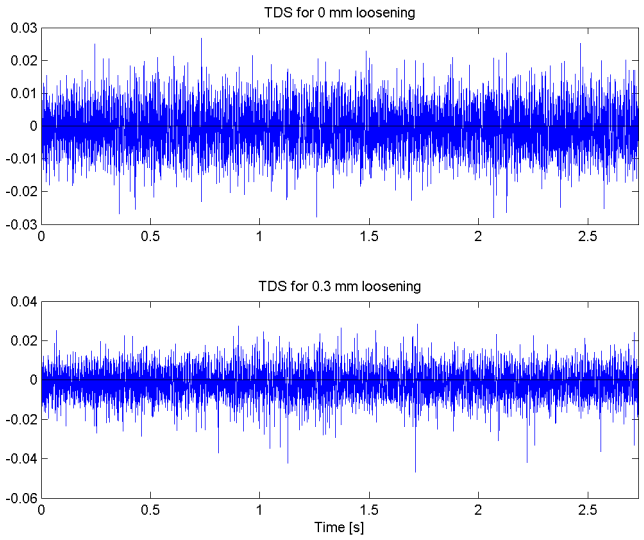

Fig. 5. Raw data recorded from the shaker between 0 s and 0.1 s for TDS at 0 and 0.3 mm of loosenning. The standard skeness is not sufficient to reveal that the signal is asymmetric at 0.3 mm loosening. The units for the y-axis have been normalized.

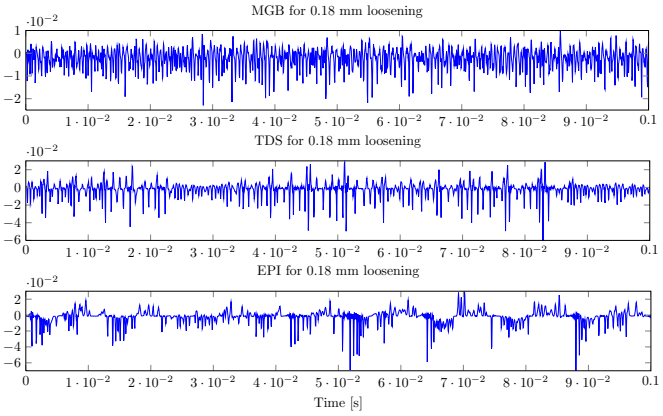

Fig. 6. Data recorded at the limit spacing: 0.18mm. The units for the y-axis have been normalized.

First evidences of failures appear at 190 cm for the TDS sensor in figure 9.

For the height of falling 190cm and 230cm, a step clearly appears at 0.3s. It is followed by a decreasing exponential evolution with a characteristic time of 0.2s. The step appears at the same time and it's amplitude increases after the 230cm experiment. That may indicate that the failure induced by the falling is activated by a special pattern that occurs in the vibrations.

4.2 In-flight recordings

One example of in-flight loosening is now presented on a helicopter equipped with 4 accelerometers, 2 mounted on the main gearbox (MGB1 and MGB2) and 2 mounted on the tail drive shaft (TDS1 and TDS2). For this aircraft, 350 recordings have been made during various flight stages (steady flight, hover, turn) and each recording contains 50000 samples at 15kHz. After the 137^{th} recording, one maintenance action has been taken on the helicopter. After

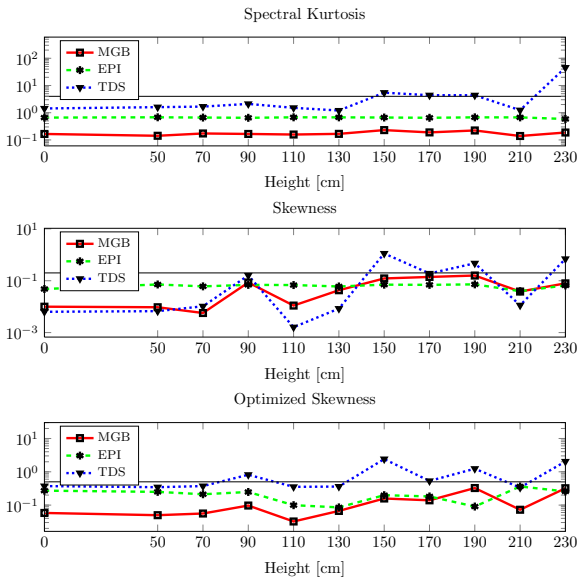

Fig. 7. Spectral Kurtosis, Skewness and Optimized Skewness in log-scale for falling experiment. Heights are in cm and the accelerometer has been replaced by an healthy one at 190 cm to avoid cumulative fault. Thresholds are plotted in solid line.

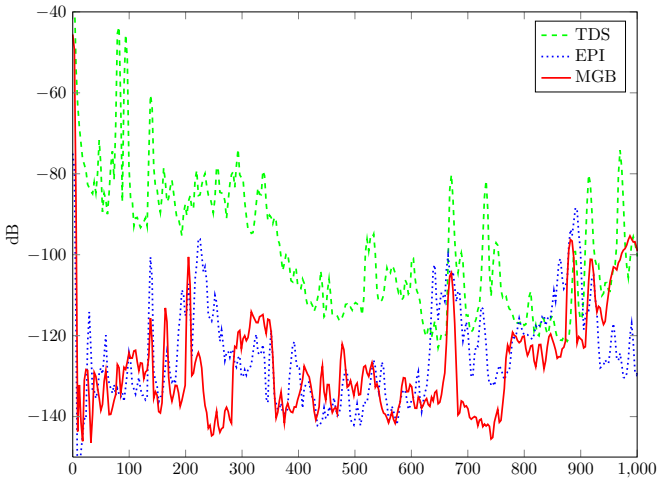

Fig. 8. Power spectral density of the original raw data for the 3 sensors.

that event, MGB2 and TDS2 triggered several HUMS alarms on all of the indicators (including crest-to-crest factor, RMS...). After verifications, it appeared that these two sensors were under-screwed. The results of the skewness and the optimised skewness are displayed in figure 10.

The optimized skewness is suddenly increasing the MGB2 and TDS2 in graphic (a) of figure 10 after the maintenance action. Before the action maintenance MGB2 is distributed around 0.1 and is distributed around 1.2 after. TDS2 is distributed around 0.1 before and around 1 after. Meanwhile, MGB1 and TDS1 are continuously distributed around 0.01 and 0.1 respectively. Since 0.5 separates the lowest value of the optimized skewness of MGB2 and TDS2 after 137 and the highest value of the optimized skewing corresponding to healthy sensors, then the threshold used for the experiments with shaker can be

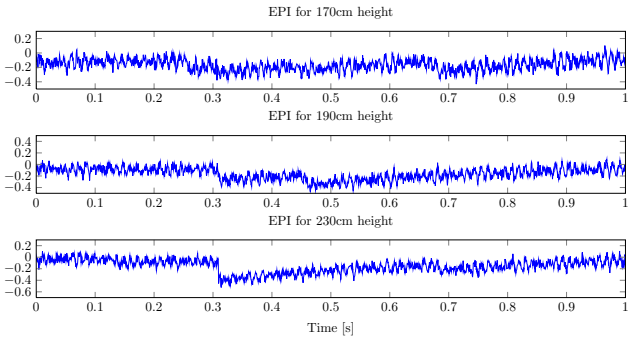

Fig. 9. Vibrations for TDS signals at 3 increasing heigth's fall. For intellectual property issues units for the y-axis have been changed and removed.

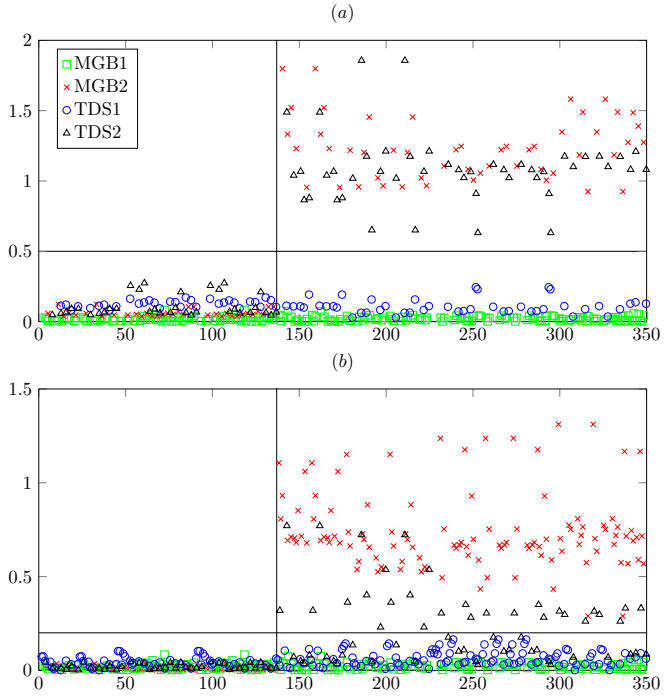

Fig. 10. Optimized skewness (a) and standard skewness (b) on MGB1, MGB2 (main gearbox) and TDS1, TDS2 for 3 consecutive days. One maintenance action has been applied after the 137^{th} recording (dotted vertical line) and produced loosening. The threshlods used in 4.1 have been plotted with solid horizontal lines: 0.5 and 0.2.

applied. The difference between the lowest and the highest values is approximately 0.3. Consequently there are no non-detection and no false-alarms with that threshold in figure 10.

The step change induced by the maintenance action is also clear for the standard skewness, however the dispersion of abnormal skewness for TDS2 overlaps the normal values of skewness of all the sensors. The results are better for MGB1 as it is possible to distinguish the skewness corresponding to the unhealthy case from the normal skewness. However the difference between the lowest value of abnormal skewness of MGB2 and the highest values of skewness of healthy indicators is about 0.15. That is twice bigger than for the optimized skewness that works that all the sensors. It is impossible to find a threshold without non-detection and without false-alarms.

Consequently the optimized skewness is preferred, since unlikely skewness it permits to separate without false alarms the faulty sensors from the others with a widest gap between the normal and the abnormal values of the indicator.

Furthermore it has been observed on other flight sets, that when the accelerometers are not well calibrated, they may saturate. When that saturation is not detected and this sensor is loosened, the skewness indicators are not efficient any more. Actually, the saturation limits the abnormal values and then limits the skewness. Using the approximation of equation 2 the relative drop in skewness is about:

$$\sqrt{2/\pi} \int_{M/\sigma}^{\infty} \exp\left(\frac{x^2}{2\sigma^2}\right) dx \tag{4}$$

When the saturation is M and the standard deviation is σ.

5. CONCLUSION

In this paper we have presented the optimized skewness to detect effects of loosening and mechanical shocks from accelerometers signals in helicopter flight context. The presented algorithm detects the presence of asymmetry in the raw data and needs 3 parameters: filter's length, fault's typical duration and one threshold. Experimental and flight test cases have been submitted to the algorithm. The optimized skewness successfully detected loosening for saturation-free recordings and showed better performances than the standard skewness. Performances on mechanical shocks are too unsteady to validate the indicator for that kind of fault. However, when the component affected by the fault is a passive element, the measured signal reflects the fault only for particular vibrations. The consequence is that the fault will not be detected when these vibrations are not received.

ACKNOWLEDGEMENTS

The authors would like to thanks J.F. Brunel and the mechanical engineering staff of Polytech'Lille for their help and support.

REFERENCES

Jerome Antoni. Fast computation of the kurtogram for the detection of transient faults. *Mechanical Systems and Signal Processing*, 21(1):108 – 124, 2007. ISSN 0888-3270.

Blinnikov and Moessner. Expansions for nearly gaussian distributions. *Astronomy and Astrophysics*, 130:193–205, 1998.

H. Endo and R.B. Randall. Enhancement of autoregressive model based gear tooth fault detection technique by the use of minimum entropy deconvolution filter. *Mechanical Systems and Signal Processing*, 21(2):906 – 919, 2007. ISSN 0888-3270.

J. Y. Lee and A. K. Nandi. Extraction of impacting signals using blind deconvolution. *Journal of Sound and Vibration*, 232(5):945 – 962, 2000. ISSN 0022-460X.

Serridge and Torben. *Accelerometres piezoelectriques et preamplificateurs de vibration Theorie et applications*. Bruel&Kjaer, 1988.

R.M. Stewart. Some useful data analysis techniques for gearbox diagnostics. Technical Report MHM/R/10/77, University of Southampton, 1977.